PROCEEDINGS OF SCIENCE

Theoretical models in nuclear astrophysics

Pierre Descouvemont[*†]
Physique Nucléaire Théorique et Physique Mathématique, C.P. 229,
Université Libre de Bruxelles (ULB), B 1050 Brussels, Belgium
E-mail: pdesc@ulb.ac.be

We review different models used in nuclear astrophysics. Definitions of the relevant cross sections and reaction rates are presented. In particular the role of the R-matrix theory and of microscopic cluster models is emphasized. We discuss three applications: R-matrix fits of the ^{12}C$(\alpha,\gamma)^{16}$O $E2$ S factor, microscopic cluster calculations of the ^{7}Be(p,γ)^{8}B reactions, and recent results on ^{2}H$(d,\gamma)^{4}$He, ^{2}H$(d,p)^{3}$H and ^{2}H$(d,n)^{3}$He obtained with realistic nucleon-nucleon interactions. These $d+d$ cross sections show evidence for an important role of the tensor force in $A=4$ systems.

XXXIV edition of the Brazilian Workshop on Nuclear Physics,
5-10 June 2011
Foz de Iguaçu, Parana state, Brazil

[*]Speaker.
[†]Directeur de Recherches FNRS.

© Copyright owned by the author(s) under the terms of the Creative Commons Attribution-NonCommercial-ShareAlike Licence.

PoS(XXXIV BWNP)008

1. Introduction

Nuclear reactions determine the nucleosynthesis in stars, and produce the energy released to compensate their gravitational contraction [1, 2, 3, 4, 5]. Stellar models are in general based on large reaction networks, involving many reaction rates. In the Big Bang nucleosynthesis, only a few reactions are important, producing elements up to $A = 8$. In stellar nucleosynthesis, the reaction networks depend on the physical conditions of the star (mass, temperature, density, etc.). At low temperatures, the stellar evolution is mainly determined by the pp chain and by the CNO cycle. Both processes convert hydrogen in Helium. Advanced stages of stellar evolution involve He burning, followed by reactions involving heavier elements. At high temperature, neutron capture (*s* and *p* processes), as well as explosive burning determine the star evolution [6, 7].

The calculation of the reaction rates relies on the cross sections. There are in general two main problems in nuclear astrophysics: (i) the stellar energies being much smaller than the Coulomb barrier, the relevant cross sections between charged particles are too small to be measured in the laboratory; (ii) explosive burning involves short-live nuclei which, even if they can be produced with modern technologies, are available with weak intensities only. Consequently a theoretical support is necessary, either to extrapolate the cross sections down to astrophysical energies, or to predict unknown cross sections.

The important processes in nuclear astrophysics are essentially capture reactions (where a nucleon or an α particle fuses with an heavier nucleus by the electromagnetic interaction), and transfer reactions (where the projectile and the target exchange nucleons). Typical examples are the ^{12}C$(\alpha,\gamma)^{16}$O and ^{13}C(α,n)^{16}O reactions, respectively. In both processes, a distinction should be made between non-resonant reactions, where the cross section does not present maxima, and resonant reactions, where the reaction rate is mainly determined by the properties of one (or more) resonance. This large variety of different situations is one of the difficulties of nuclear astrophysics, since no systematics can be used. Particularly in low-mass nuclei, each reaction presents its own specificities, and must be treated individually [8].

Theoretical models used in nuclear astrophysics can be roughly classified in three categories [8, 9]:

(i) Models involving adjustable parameters, such as the *R*-matrix method [10, 11]; parameters are fitted to the available experimental data and the cross sections are extrapolated down to astrophysical energies. These fitting procedures of course require the knowledge of data, which are sometimes too scarce for a reliable extrapolation.

(ii) "Non fitting" models, where the cross sections are determined from the wave functions of the system. The potential model [12], the Distorted Wave Born Approximation (DWBA) [13], and microscopic models [14, 15] are, in principle, independent of experimental data. More realistically, these models depend on some physical parameters, such as a nucleus-nucleus or a nucleon-nucleon interaction which can be reasonably determined from experiment only. The microscopic Generator Coordinate Method (GCM) provides a "basic" description of a *A*-nucleon system, since the whole information is obtained from a nucleon-nucleon interaction. Since this interaction is nearly the same for all light nuclei, the predictive power of the GCM is important.

(iii) Models (i) and (ii) can be used for low level-density nuclei only. This condition is fulfilled in most of the reactions involving light nuclei ($A \leq 20$). However when the level density near

PoS(XXXIV BWNP)008

threshold is large (i.e. more than a few levels per MeV), statistical models, using averaged optical transmission coefficients, are in general more suitable [16, 17]. In some specific applications, shell-model theories can provide the gamma widths of relevant states [18].

Our goal here is to discuss the importance of nuclear reactions in astrophysics. We essentially focus on reaction cross sections, and on resonance properties. In Section 2, we present the general definitions of cross sections and reaction rates. A clear distinction is made between resonant and non-resonant reactions. Section 3 is devoted to a brief description of various models used in low-energy nuclear physics. In particular the *R*-matrix method (extrapolation) and cluster models are briefly reviewed. Recent examples are presented in Section 4, and concluding remarks in Section 5.

2. Cross sections and reaction rates

2.1 Cross sections

Reactions relevant in nuclear astrophysics are essentially transfer and radiative capture reactions [8]. They arise from the nuclear and electromagnetic interactions, respectively. As a consequence, transfer cross sections are much larger than capture cross sections, which are negligible unless the transfer channel is closed. For the sake of completeness, let us mention that two electroweak reactions also play a role [19]: $p(p,e^+\nu)d$ is the first stage of hydrogen burning, and ^{3}He$(p,e^+\nu)^4$He produces high-energy neutrinos. Both reactions arise from the weak interaction, and therefore present tiny cross sections at stellar energies, inaccessible in current experiments.

Let us first discuss capture cross sections. A radiative transition is an electromagnetic process where two colliding nuclei at energy E fuse to a final state $(J_f\pi_f)$ of the unified nucleus at energy E_f. The capture cross section is given, in the first-order perturbation theory, by a matrix element of the electromagnetic Hamiltonian. This operator is expanded in electric ($\sigma = E$) and magnetic ($\sigma = M$) multipole operators $\mathscr{M}^\sigma_{\lambda\mu}$. The cross section between nuclei with spins I_1 and I_2, integrated over all photon directions, then reads

$$\sigma_c(E,J_f\pi_f) = \frac{2J_f+1}{(2I_1+1)(2I_2+1)} \sum_{\sigma\lambda J_i I\ell_i} \frac{1}{2\ell_i+1} \frac{8\pi(\lambda+1)}{\hbar\lambda(2\lambda+1)!!^2} k_\gamma^{2\lambda+1} \times |<\Psi^{J_f\pi_f}||\mathscr{M}^\sigma_\lambda||\Psi^{J_i\pi_i}_{\ell_i I}(E)>|^2, \quad (2.1)$$

where $k_\gamma = (E-E_f)/\hbar c$ is the photon wave number and $\Psi^{J_i\pi_i}_{\ell_i I}(E)$ is a partial wave of a unit-flux scattering wave function [8]. The wave function of the final bound state is denoted as $\Psi^{J_f\pi_f}$. In practice, owing to the electromagnetic selection rules and to the low energies, only a few terms contribute.

The transfer cross section from an initial channel i to a final channel f is derived from the collision (or scattering) matrix $U^{J\pi}$ as

$$\sigma_t(E,i\to f) = \frac{\pi}{k^2} \sum_{J\pi} \frac{2J+1}{(2I_1+1)(2I_2+1)} \sum_{\ell\ell' II'} |U^{J\pi}_{i\ell I,f\ell' I'}(E)|^2, \quad (2.2)$$

where k is the wave number of the relative motion, and (ℓI) are the orbital momentum and the channel spin, respectively. These definitions are common to all models. In the following we will be more specific and consider various theoretical approaches.

PoS(XXXIV BWNP)008

As stellar energies are much lower than the Coulomb barrier, the cross sections strongly depend on energy. The fast energy dependence of the cross section at sub-Coulomb energies is partly removed in the *S*-factor, defined as

$$S(E) = \sigma(E) E \exp(2\pi\eta), \tag{2.3}$$

where $\eta = Z_1 Z_2 e^2/\hbar v$ is the Sommerfeld parameter. For non-resonant reactions, the *S*-factor smoothly depends on energy and contains the nuclear information on the reaction. Whereas the cross section varies by several orders of magnitude in the experimental energy range, the *S* factor weakly depends on energy.

2.2 Reaction rates

The main nuclear inputs in stellar models are the reaction rates $< \sigma v >$, where v is the relative velocity between the colliding nuclei [2]. Production and destruction of nuclear species are given by a set of coupled differential equations involving the reaction rates, and providing abundances of each element at given time and temperature. The reaction rate is known to be strongly dependent on the presence or absence of resonances. In both situations, analytical approximations can be derived.

Let us consider a reaction between two nuclei with masses $A_1 m_N$ and $A_2 m_N$ and charges $Z_1 e$ and $Z_2 e$ (we express here the masses in units of the nuclear mass m_N). The reaction rate at temperature T is defined as [1, 2]

$$N_A < \sigma v > = N_A \left(\frac{8}{\pi \mu m_N (k_B T)^3} \right)^{\frac{1}{2}} \int \sigma(E) E \exp(-E/k_B T) dE, \tag{2.4}$$

where we assume that the star can be considered as a perfect gas following the Maxwell-Boltzmann distribution. In Eq. (2.4), N_A is the Avogadro number, $\mu = A_1 A_2/(A_1 + A_2)$ is the dimensionless reduced mass, and k_B is the Boltzmann constant. At sub-coulomb energies the astrophysical *S* factor is almost constant, and the energy dependence of the cross section varies as

$$\sigma(E) \sim \exp(-2\pi\eta)/E. \tag{2.5}$$

Using (2.5), the integrand of (2.4) can be approximated by a Gaussian shape [1, 2] with a maximum at the Gamow peak. The energy and width of the peak are given by

$$E_0 = \left[\pi \frac{e^2}{\hbar c} Z_1 Z_2 k_B T (\mu m_N c^2/2)^{1/2} \right]^{2/3} \approx 0.122\, \mu^{1/3} (Z_1 Z_2 T_9)^{2/3} \text{ MeV}, \tag{2.6}$$

$$\Delta E_0 = 4(E_0 k_B T/3)^{\frac{1}{2}} \approx 0.237\, (Z_1^2 Z_2^2 \mu)^{1/6} T_9^{5/6} \text{ MeV}, \tag{2.7}$$

where T_9 is the temperature expressed in $10^9 K$. The Gamow energy defines the energy range where the cross section needs to be known to derive the reaction rate. Resonance properties must also be available in this energy range. In most cases, this energy is much lower than the Coulomb barrier V_B which means that the cross sections drop to very low values. The width ΔE_0 is small at low energies, and in low-mass nuclei. However, at high temperatures, typical of explosive burning, ΔE_0 becomes quite large. In that case, properties of many resonances should be known. Table 1 gives

PoS(XXXIV BWNP)008

Table 1: Typical Gamow-peak energies and widths. V_B is the energy of the Coulomb barrier.

Reaction	T_9	E_0 (MeV)	ΔE_0 (MeV)	V_B (MeV)	$\sigma(E_0)/\sigma(V_B)$
d+p	0.015	0.006	0.007	0.70	7.0×10^{-3}
^{3}He+^{3}He	0.015	0.021	0.012	1.4	1.1×10^{-11}
α+^{12}C	0.2	0.31	0.17	3.2	4.9×10^{-11}
^{12}C+^{12}C	1	2.41	1.05	8.1	2.3×10^{-11}

some typical values. The ratio $\sigma(E_0)/\sigma(V_B)$ has been obtained by assuming a constant S-factor; it shows how fast the cross section decreases from the Coulomb barrier down to astrophysical energies.

Rigorously the reaction rate should be calculated numerically by using experimental or theoretical cross sections. However, the analytical approach provides a more intuitive understanding of the physics, and is still widely used. Let us start with non-resonant reactions, where the S-factor weakly depends on energy. In this case, the integral (2.4) can be replaced by an accurate analytical approximation. A Taylor expansion near E_0 provides

$$\exp(-2\pi\eta - E/k_BT) \approx \exp(-3E_0/k_BT)\exp\left(-\left(\frac{E-E_0}{\Delta E_0/2}\right)^2\right). \tag{2.8}$$

Assuming a linear variation of $S(E)$ in the Gamow peak [2], the reaction rate is then given by

$$N_A<\sigma v> \approx N_A\left(\frac{32E_0}{3\mu m_N(k_BT)^3}\right)^{\frac{1}{2}}\exp\left(-\frac{3E_0}{k_BT}\right)\left(1+\frac{5k_BT}{36E_0}\right)S(E_0+\frac{5}{6}k_BT), \tag{2.9}$$

which presents a fast variation with temperature, owing to the exponential term.

For resonant reactions in partial wave J_R at energy E_R, the cross section is assumed to have a Breit-Wigner form, valid near $E=E_R$,

$$\sigma(E) \approx \frac{\pi}{k^2}\frac{2J_R+1}{(2I_1+1)(2I_2+1)}\frac{\Gamma_1(E)\Gamma_2(E)}{(E-E_R)^2+\Gamma(E)^2/4}, \tag{2.10}$$

where Γ_1 and Γ_2 are the partial widths in the entrance and exit channels ($\Gamma=\Gamma_1+\Gamma_2$). This definition is common to capture and to transfer reactions. In the former case, Γ_2 is the γ width of the resonance, while in the latter case, it corresponds to a particle width. For resonant reactions, the general definition (2.4) is of course still valid. However, one has to account for the fast variation of $S(E)$ near the resonance energy. Since a numerical approach is difficult for narrow resonances, we present an analytical method, widely used in nuclear astrophysics.

A careful analysis of integrand (2.4) shows that it always presents two maxima [8]: at the resonance energy, and at the Gamow energy. The peak at the resonance energy does not depend on temperature. The second peak, corresponding to the Gamow energy, moves according to the temperature. From these considerations, and except in the temperature range where both peaks overlap, the resonant reaction rate can be split in two terms

$$N_A<\sigma v> \approx N_A<\sigma v>_R + N_A<\sigma v>_T, \tag{2.11}$$

PoS(XXXIV BWNP)008

where $N_A < \sigma v >_R$ corresponds to the maximum at $E = E_R$. For a narrow resonance, we have

$$N_A < \sigma v >_R = N_A \left(\frac{2\pi}{\mu m_N k_B T} \right)^{\frac{3}{2}} \hbar^2 \omega\gamma \exp\left(-\frac{E_R}{k_B T} \right), \tag{2.12}$$

where the resonance strength $\omega\gamma$ is defined by

$$\omega\gamma = \frac{2J_R+1}{(2I_1+1)(2I_2+1)} \frac{\Gamma_1\Gamma_2}{\Gamma_1+\Gamma_2}, \tag{2.13}$$

(Γ_1, Γ_2) being the partial widths at $E = E_R$. In capture reactions, the γ width is in general much lower than the particle width. The resonance strength is then proportional to the smaller partial width $\Gamma_2 = \Gamma_\gamma$. The second maximum of integrand (2.11) yields the so-called "tail resonance" term $N_A < \sigma v >_T$. Its analytical expression is identical to the non-resonant rate (2.9) with a Breit-Wigner expression for $S(E)$.

3. Theoretical models

3.1 Introduction

As mentioned before, reaction models are essential in nuclear astrophysics. Many models have been used to describe low-energy reactions. Here we give a brief overview of various approaches, commonly used in nuclear astrophysics.

3.2 Microscopic cluster theories

Microscopic models are based on fundamental principles of quantum mechanics, such as the treatment of all nucleons, with exact antisymmetrization of the wave functions. Neglecting three-body forces, the Hamiltonian of a A-nucleon system is written as

$$H = \sum_{i=1}^{A} T_i + \sum_{i<j=1}^{A} V_{ij}, \tag{3.1}$$

where T_i is the kinetic energy and V_{ij} a nucleon-nucleon interaction [14].

The Schrödinger equation associated with this Hamiltonian can not be solved exactly when $A > 3$. For very light systems ($A \sim 4-5$) efficient methods [20] exist, even for continuum states [21]. However most reactions relevant in nuclear astrophysics involve heavier nuclei essentially with nucleon or α projectiles. Recent developments of *ab initio* models (see for example Refs. [22, 23, 24]) are quite successful for spectroscopic properties of low-lying states. These models make use of realistic interactions, including three-body forces, and fitted on many properties of the nucleon-nucleon system. Recent works succeeded in computing the ^{3}He$(\alpha,\gamma)^7$Be [23] and ^{2}H$(d,\gamma)^4$He [25] cross sections from realistic interactions. However, a consistent description of bound and scattering states of an A-body problem remains a very difficult task [21], in particular for transfer reactions.

In cluster models, it is assumed that the nucleons are grouped in clusters [14, 26]. We present here the specific application to two-cluster systems. The internal wave functions of the clusters are

PoS(XXXIV BWNP)008

denoted as $\phi_i^{I_i\pi_i\nu_i}(\xi_i)$, where I_i and π_i are the spin and parity of cluster i, and ξ_i represents a set of their internal coordinates. A channel function is defined as

$$\varphi_{\ell I}^{JM\pi}(\Omega_\rho,\xi_1,\xi_2) = \left[Y_\ell(\Omega_\rho)\otimes[\phi_1^{I_1\pi_1}(\xi_1)\otimes\phi_2^{I_2\pi_2}(\xi_2)]^I\right]^{JM}, \tag{3.2}$$

where different quantum numbers show up: the channel spin I, the relative angular momentum ℓ, the total spin J and the total parity $\pi=\pi_1\pi_2(-)^\ell$.

The total wave function of the A-nucleon system is written as

$$\begin{aligned}\Psi^{JM\pi} &= \sum_{\alpha\ell I}\Psi_{\alpha\ell I}^{JM\pi} \\ &= \sum_{\alpha\ell I}\mathscr{A}\, g_{\alpha\ell I}^{J\pi}(\rho)\ \varphi_{\alpha\ell I}^{JM\pi}(\Omega_\rho,\xi_1,\xi_2),\end{aligned} \tag{3.3}$$

which corresponds to the Resonating Group (RGM) definition [27, 28, 26]. Index α refers to different two-cluster arrangements, and $\mathscr{A}$ is the antisymetrization operator. In most applications, the internal cluster wave functions $\phi_i^{I_i\pi_i\nu_i}$ are defined in the shell model. Accordingly, the nucleon-nucleon interaction must be adapted to this choice, which leads to effective forces, such as the Volkov [29] or the Minnesota [30] interactions. The relative wave functions $g_{\alpha\ell I}^{J\pi}(\rho)$ are to be determined from the Schrödinger equation, which is transformed into a integro-differential equation involving a non-local potential [28]. In most applications, this relative function is expanded over Gaussian functions [14, 26], which corresponds to the Generator Coordinate Method (GCM). The wave function (3.3) is rewritten as

$$\Psi_{\alpha\ell I}^{JM\pi} = \int f_{\alpha\ell I}^{J\pi}(R)\Phi_{\alpha\ell I}^{JM\pi}(R), \tag{3.4}$$

where $\Phi_{\alpha\ell I}^{JM\pi}(R)$ is a projected Slater determinant, and $f_{\alpha\ell I}^{J\pi}(R)$ the generator function, which must be determined. The GCM is equivalent to the RGM, but is better adapted to numerical calculations, as it makes uses of projected Slater determinants (see Ref. [14, 26] for detail).

The main advantage of cluster models with respect to other microscopic theories is their ability to deal with reactions, as well as with nuclear spectroscopy. The first applications were done for reactions involving light nuclei, such as d, ^{3}He or α particles [31, 32]. More recently, much work has been devoted to the improvement of the internal wave functions: multicluster descriptions [33], large-basis shell model extensions [34], or monopolar distortion [35].

As mentioned before, the RGM radial wave functions are expanded over a Gaussian basis. The GCM is well adapted to numerical calculations, and to a systematic approach, but the Gaussian behaviour is not physical at large distances, and must be corrected. We use the Microscopic R-matrix Method (MRM) [36, 11] which is a direct extension of the standard R-matrix technique [10], based on the existence of two regions: the internal region (with channel radius a), where the nuclear force and the nucleus-nucleus antisymmetrization are important, and the external region where they can be neglected. In the external region, the Gaussian behaviour of the RGM radial function is replaced by Coulomb functions. Matching the internal and external components provide, either the collision matrix for scattering states, or the binding energy for bound states.

PoS(XXXIV BWNP)008

3.3 The potential model

Solving the Schrödinger equation associated with the Hamiltonian (3.1) is in general a difficult problem, which does not have an exact solution when the nucleon number is larger than three. The potential model is fairly simple to use, and has been applied to many reactions in low-energy nuclear physics [37, 12, 38, 39, 40]. The basic assumptions of the potential model are: (i) the nucleon-nucleon interaction is replaced by a nucleus-nucleus force $V(\rho)$, which depends on the relative coordinate ρ only; (ii) the wave functions of the unified nucleus can be described by a cluster structure with A_1+A_2 nucleons; (iii) the internal structure of the nuclei does not play any role. Since we are dealing with low energies, the potential is in general real. The extension to higher energies, which requires complex potentials to simulate absorption channels, is known as the optical model. A generalization to coupled-channel problems is also possible, but seldom used in nuclear astrophysics.

The radial function $g_{\ell J}^{J\pi}(\rho)$ for bound and scattering states is deduced from the equation

$$\left(-\frac{\hbar^2}{2\mu m_N}\left(\frac{d^2}{dr^2}-\frac{\ell(\ell+1)}{r^2}\right)+V(\rho)\right)g_{\ell J}^{J\pi}(\rho)=E\,g_{\ell J}^{J\pi}(\rho), \tag{3.5}$$

where E is the relative energy ($E>0$ for scattering states and $E<0$ for bound states). Let us notice that the potential may depend on ℓ and J. In nuclear physics, the nucleus-nucleus potential involves a Coulomb term $V_C(\rho)$ and a nuclear term $V_N(\rho)$. According to the application, the choice of the nuclear contribution is guided by experimental constraints. In radiative-capture calculations it is crucial to reproduce the final-state energy. If phase shifts are available, they can be used to determine the initial potential.

In this simple model, the capture cross section (2.1) is deduced from integrals involving scattering functions $g_{\ell_i I}^{J_i\pi_i}(\rho)$ at energy E, and bound-state wave functions $g_{\ell_f I}^{J_f\pi_f}(\rho)$. For an electric multipole of order λ it is given by

$$\sigma_c(E,J_f\pi_f) = 8\pi\frac{e^2}{\hbar v k^2}\left[Z_1\left(\frac{A_2}{A}\right)^\lambda+Z_2\left(\frac{-A_1}{A}\right)^\lambda\right]^2 k_\gamma^{2\lambda+1}\frac{(\lambda+1)(2\lambda+1)}{\lambda[(2\lambda+1)!!]^2} \tag{3.6}$$

$$\times\sum_{J_i,I,\ell_i}\frac{(2\ell_f+1)(2J_f+1)(2J_i+1)}{(2I_1+1)(2I_2+1)}<\ell_f 0\lambda 0|\ell_i 0>^2$$

$$\times\left\{\begin{array}{ccc} J_i & \ell_i & I \\ \ell_f & J_f & \lambda\end{array}\right\}^2\left(\int_0^\infty g_{\ell_i I}^{J_i\pi_i}(\rho)\rho^\lambda g_{\ell_f I}^{J_f\pi_f}(\rho)\,d\rho\right)^2. \tag{3.7}$$

In this definition, the amplitude of the scattering state is

$$g_{\ell_i I}^{J_i\pi_i}(\rho)\underset{\rho\to\infty}{\longrightarrow}F_{\ell_i}(k\rho)\cos\delta_{\ell_i I}^{J_i\pi_i}+G_{\ell_i}(k\rho)\sin\delta_{\ell_i I}^{J_i\pi_i}, \tag{3.8}$$

where $F_\ell(x)$ and $G_\ell(x)$ are the Coulomb functions, and $\delta_{\ell_i I}^{J_i\pi_i}$ the phase shift. The bound-state wave function is normalized to unity and tends to

$$g_{\ell_f I}^{J_f\pi_f}(\rho)\underset{\rho\to\infty}{\longrightarrow}C_{\ell_f I}^{J_f\pi_f}W_{-\eta_f,\ell_f+1/2}(2k_f\rho), \tag{3.9}$$

where $W(x)$ is the Whittaker function, and k_f and η_f the wave number and Sommerfeld parameter of the bound state. In Eq. (3.9), $C_{\ell_f I}^{J_f\pi_f}$ is the Asymptotic Normalization Constant (ANC). It plays a

PoS(XXXIV BWNP)008

crucial role for transitions to weakly bound states [41]. In this situation, the exponential decrease of the bound-state wave function is very slow, and the main contribution to the integral in (3.7) arises from large distances. Consequently the cross section is essentially determined by the ANC. A typical example is the ^{7}Be(p,γ)^{8}B reaction [42], where the final ^{8}B ground state is bound by 137 keV only.

3.4 The phenomenological *R*-matrix method

The *R*-matrix method is well known in atomic and nuclear physics [11]. The basis idea is to divide the space in two regions: the internal region (with radius a), where the nuclear force is important, and the external region, where the interaction between the nuclei is governed by the Coulomb force only. Although the *R*-matrix parameters do depend on the channel radius a, the sensitivity of the cross section with respect to its choice is quite weak. In the *R*-matrix method, the energy dependence of the cross sections is obtained from Coulomb functions, as expected from the Schrödinger equation.

The physics of the internal region is determined by a number N of poles, which are characterized by energy E_λ and reduced widths $\gamma_{\lambda i}$. In a multichannel problem, the *R*-matrix at energy E is defined as

$$R_{if}(E) = \sum_{\lambda=1}^{N} \frac{\gamma_{\lambda i}\gamma_{\lambda f}}{E_\lambda - E}, \tag{3.10}$$

which must be given for each partial wave J (not written for the sake of clarity). Indices i and f refer to the initial and final channels. The pole properties are associated with the physical energy and width of resonances, but not strictly equal. This is known as the difference between “formal" and “observed" parameters, deduced from experiment. In a general case, involving more than one pole, the link between those two sets is not straightforward (see Refs. [43, 44] for a general formulation of this problem). The collision matrix, and therefore the cross sections, are directly determined from the *R* matrices in the different partial waves (see Refs. [10, 11]).

The method can be applied in two ways: (i) in the *calculable* *R*-matrix, parameters E_λ, $\gamma_{\lambda i}$ and $\gamma_{\lambda f}$ are obtained from a variational calculation; (ii) in the *phenomenological* *R*-matrix variant, these quantities are fitted to experiment. The calculable *R*-matrix method is used, for example in microscopic calculations (see section 3.2). Variational methods are widely used in physics; they rely on the choice of square-integrable basis functions, which tend to zero at large distances. The correct Coulomb behaviour can be restored by using these basis functions in the internal region, and the asymptotic behaviour (3.8) in the external region (see Ref. [11] for a review and recent applications). In general this method is quite efficient in scattering problems: coupled-channel theories, three-body problems, microscopic calculations, etc. Many applications exist in atomic and in nuclear physics.

Although the origin of the phenomenological variant is identical, its application is somewhat different. In nuclear astrophysics the main goal of the *R*-matrix method [10] is to parameterize some experimentally known quantities, such as cross sections or phase shifts, with a small number of parameters, which are then used to extrapolate the cross section down to astrophysical energies. A well known example is the ^{12}C(α,γ)^{16}O reaction, which has been studied by many groups. In spite of impressive experimental efforts, the lowest experimental energies are around 0.8 MeV, whereas

PoS(XXXIV BWNP)008

the Gamow peak (at the typical He-burning temperature $T_9 = 0.2$) is $E_0 \approx 0.3$ MeV. At these subcoulomb energies, the cross sections drop by several orders of magnitude, and extrapolation techniques are necessary. We refer to Refs. [45] for recent works on this topic.

The *R*-matrix method can be applied to transfer as well as to capture reactions. It is usually used to investigate resonant reactions but is also suited to describe non-resonant processes [46]. In the latter case, the non-resonant behavior is simulated by a high-energy pole, referred to as the background contribution, which makes the *R*-matrix nearly energy independent.

4. Specific examples

4.1 *R*-matrix parameterizations of the ^{12}C$(\alpha,\gamma)^{16}$O $E2$ cross section

The ^{12}C$(\alpha,\gamma)^{16}$O reaction plays a major role in nuclear astrophysics [47], as it determines the ^{12}C/^{16}O ratio after helium burning. In the nuclear physics point of view, the ^{12}C$(\alpha,\gamma)^{16}$O cross section is very difficult for several reasons. The Gamow energy (≈ 300 keV at the typical He-burning temperature $T = 2\times10^8$ *K*) is much lower than the Coulomb barrier, and the cross section cannot be measured at stellar energies [2]. The $E1$ multipolarity, although forbidden at the long wavelength limit in $N = Z$ nuclei, does not vanish owing to isospin impurities, and to the presence of a 1^- broad resonance near 2.5 MeV. A further specificity of the ^{12}C$(\alpha,\gamma)^{16}$O cross section is the presence, in both multipolarities, of a subthreshold state (1^-_1 at $E_{\rm c.m.} = -45$ keV for $E1$, and 2^+_1 at $E_{\rm c.m.} = -245$ keV for $E2$) whose effect is dominant at stellar energies, but less important in the experimental range. In addition, these states interfere with higher energy resonances (1^-_2 at $E_{\rm c.m.} = 2.4$ MeV for $E1$, 2^+_2 at $E_{\rm c.m.} = 2.68$ MeV for $E2$), and interference patterns show up in the *S*-factor.

The importance of the $E2$ component in the ^{12}C$(\alpha,\gamma)^{16}$O cross section was first pointed out by Dyer and Barnes [48] in 1974. However, disentangling the $E1$ and $E2$ multipolarities requires high-precision data and, in particular, angular distributions. According to most recent estimates [49], the $E1$ and $E2$ multipolarities are of similar amplitude in the capture cross section. The goal of the present work [45] is to investigate the $E2$ multipolarity in a standard *R*-matrix analysis involving the latest experimental data.

Definition (3.10) of the *R*-matrix is used for elastic scattering. For the capture cross section, the gamma width of each pole is introduced, and the *R*-matrix theory is extended to electromagnetic transitions [11]. As usual for the *d*-wave phase shift we use $N = 4$ poles, associated with the ^{16}O states at -0.245 ($2^+_1, \lambda = 1$), 2.68 ($2^+_2, \lambda = 2$) and 4.36 MeV ($2^+_3, \lambda = 3$), complemented by a background term ($\lambda = 4$). Several properties of these states are well known experimentally, and are fixed in the *R*-matrix fits. We fit the *d*-wave phase shifts and the E2 capture data for various values of E_4.

The $E2$ *S*-factors are presented in Fig. 1 for different background energies. The experimental data sets have a limited overlap between each other, which leads to rather high χ^2 (≈ 3). This problem is well known, and arises from the experimental difficulties associated with the ^{12}C$(\alpha,\gamma)^{16}$O reaction. Fig. 1 shows that for small E_4 values the *S* factor strongly varies. Although the χ^2 values are weakly affected, $E_4 < 7$ MeV should probably be discarded. Accordingly, only an upper limit can be obtained for the extrapolated *S* factor ~ 190 keV-b.

PoS(XXXIV BWNP)008

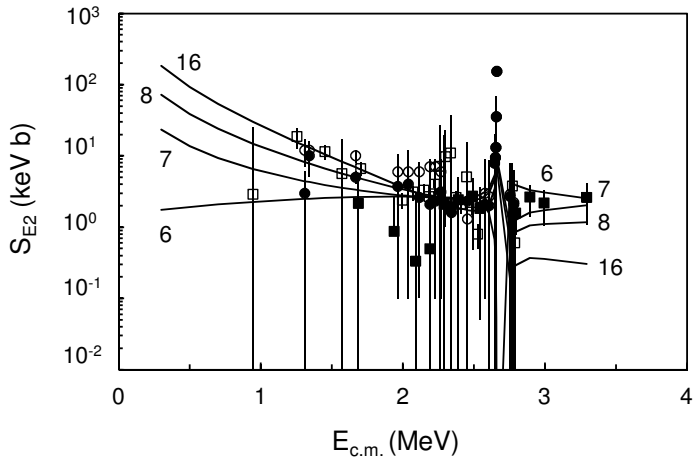

Figure 1: ^{12}C$(\alpha,\gamma)^{16}$O $E2$ S factors obtained by R-matrix fits for different background energies E_4 (labels). Experimental data are as in Ref. [45].

From the R-matrix fits we conclude that current phase-shift and capture data alone cannot provide an extrapolated S factor with a low uncertainty. This conclusion is similar to that drawn for the $E1$ multipolarity, but the ^{16}N β-decay data provide a strong constraint on the fit. For the $E2$ component, we have used the 2^+_1 ANC provided by the GCM as additional constraint (see Ref. [45]). This value is in good agreement with available data and, owing to the $\alpha+^{12}$C cluster structure, is expected to be reliable in a cluster model. This external data was shown to strongly reduce the uncertainties on the R-matrix fits. The S factor determined in this way ($S_{E2}(300\text{ keV}) = 42 \pm 2$ keV-b) is slightly lower than a microscopic cluster calculation (50 keV-b) [45], but should be more reliable as all properties of the 2^+ resonances are taken from experiment.

4.2 Application of microscopic cluster models to ^{7}Be(p,γ)^{8}B

As an example of microscopic cluster models we choose the ^{7}Be(p,γ)^{8}B S-factor, which plays a crucial role in the solar-neutrino problem [50]. Many direct as well as indirect measurements have been performed in order to reduce the uncertainties on the S-factor at zero energy (see Ref. [51] for an overview). As a high precision is required for $S(0)$, the extrapolation down to astrophysical energies should be done very carefully. Current experiments are performed in a limited energy range, which requires the use of a theoretical model to derive $S(0)$. The reliability of the model can be tested in the energy range where data exist, which provides some "confidence level" on the extrapolation. In most experiments, a microscopic cluster model [33] (hereafter referred to as DB94) is used for the extrapolation. This model takes account of the ^{7}Be deformation, of inelastic and rearrangement channels, and has been tested with spectroscopic properties of ^{8}B and ^{8}Li, as well as with the ^{7}Li(n,γ)^{8}Li mirror cross section. An update of the calculation has been performed more recently [52]. The theoretical S-factors obtained with two different nucleon-nucleon interactions (MN and V2) are shown in Figure 2.

As discussed in DB94, a cluster model provides an upper bound of the capture cross section. The "exact" ^{8}B wave function should contain many other configurations (other arrangements, 4 clusters, 5 clusters, etc.). Accordingly, the capture cross section which, up to the electromagnetic

PoS(XXXIV BWNP)008

operator, is nothing but the overlap between the initial ^{7}Be+p and final ^{8}B wave functions, is in general overestimated by a cluster model. This overestimation factor decreases as the model is improved.

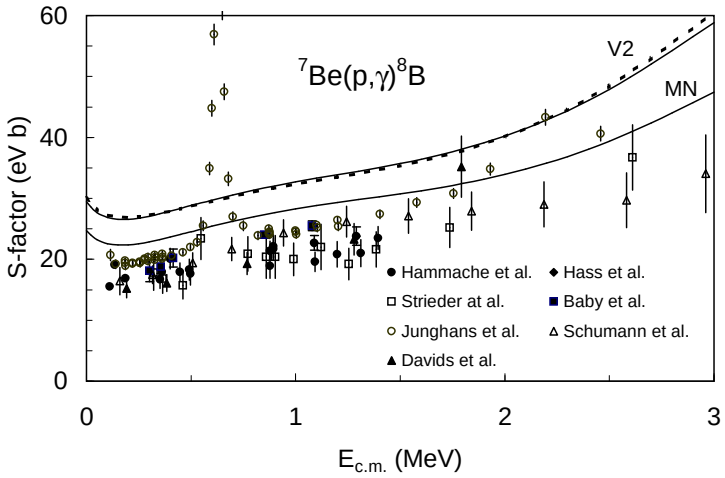

Figure 2: ^{7}Be(p,γ)^{8}B S factor with two nucleon-nucleon interactions (V2 and MN, solid lines from [52]). The results of DB94 are shown as a dashed line. See Ref. [52] for references to the data.

The $E2$ transition between the 2^+ ground state and the first excited 1^+ state in the mirror ^{8}Li nucleus is an interesting issue, and indirectly related to the ^{7}Be(p,γ)^{8}B reaction. About 20 years ago, the quadrupole (E2) excitation of ^{8}Li was measured using a radioactive beam [53, 54], and unexpectedly large $B(E2)$ values were obtained ($B(E2,2^+ \rightarrow 1^+) = 30 \pm 15\, e^2.\text{fm}^4$ and $55 \pm 15\, e^2.\text{fm}^4$). These large values cannot be explained by a microscopic three-cluster model [55] which provides much smaller $B(E2)$ ($2.1\, e^2.\text{fm}^4$), although it nicely reproduces many other properties of ^{8}Li and of similar light nuclei. This discrepancy raises a very challenging question for nuclear physicists: if confirmed the very large $B(E2)$ obtained in [53, 54] would question the precision of most nuclear models. Obviously a remeasurement of the Coulomb excitation of ^{8}Li with modern techniques is desirable.

4.3 Ab-initio calculation of the ^{2}H$(d,\gamma)^4$He, ^{2}H$(d,p)^3$H and ^{2}H$(d,n)^3$He cross sections

The knowledge of the reaction cross sections at astrophysical energies is of great interest not only for establishing imprints of the properties of nuclei in the universe but also for understanding an interplay between the structure and reactions of these nuclei based on a nucleon-nucleon (NN) interaction. Aside from the astrophysical interest, the ^{2}H$(d,\gamma)^4$He capture reaction is extremely important from the nuclear physics viewpoint because its cross section at low energies (below 0.3 MeV) is expected to be dominated by D-wave components in the α particle. Hence it should be very sensitive to the tensor force in the NN interaction [56, 15, 57].

We have recently applied a multi-channel microscopic cluster model to study the phase shifts of the p+^{3}He [58] and $d+d$, p+^{3}H, n+^{3}He [59] systems. The model combines the stochastic variational method (SVM) [60, 61] with the microscopic R-matrix theory [11]. For the ^{2}H, ^{3}H and ^{3}He nuclei, we use combinations of Gaussian functions to solve the Schrödinger equation for the

PoS(XXXIV BWNP)008

cluster intrinsic Hamiltonian [25]. The relative function between the clusters is also expanded in a Gaussian basis. Matrix elements of the Hamiltonian can be obtained analytically [59].

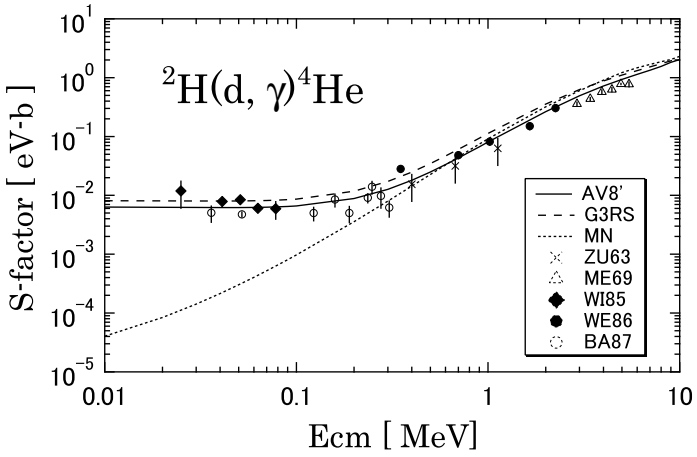

Figure 3: The astrophysical *S*-factor of ^{2}H(d, γ)^{4}He reaction. Results calculated with the realistic (AV8′, G3RS) and the effective (MN) potentials are compared to experiment (see Ref. [62]).

For the two-body *NN* interaction V_{ij} we use two different realistic potentials, AV8′ [63] and G3RS [64], that consist of central, tensor, and spin-orbit components. The latter potential is softer than the former and gives slightly smaller *D*-state probabilities in d, ^{3}H, and α [65]. It is crucial to reproduce the $d+d$, $p+^3$H, and $n+^3$He two-body thresholds for comparing calculated *S*-factors to experiment. These thresholds are fairly well reproduced by the AV8′ and G3RS realistic interactions. However, they can be still improved by including a phenomenological three-body force taken from Ref. [66]. Because our main aim is to clarify the role of the tensor force, it is useful to compare results obtained with the realistic interactions with that of an effective *NN* interaction that contains no tensor force. Using such effective interaction is reasonable because only *s*-shell nuclei participate to the reactions. We adopt the MN central potential [30] with a standard value for the admixture parameter $u = 1$. More detail can be found in Ref. [25].

Figure 3 displays the calculated astrophysical *S*-factor for the ^{2}H(d,γ)^{4}He reaction. Results with both AV8′ (solid line) and G3RS (dashed line) potentials reproduce very well the experimental data, especially its flat behavior at low energies (typical of an initial *s* wave), whereas the MN potential (dotted curve) shows a rapidly decreasing pattern as $E_{\rm cm}$ decreases.

To clarify the energy-dependence of the *S*-factor, we studied the contributions of the three incoming dd channels to the *S*-factor: $^5S_2$, $^1D_2$, and $^5D_2$ (we use the spectroscopic notation $^{2I+1}\ell_J$). Without tensor interaction the α particle only contains an $I = 0$ component and transitions from the initial $^5S_2$ and $^5D_2$ partial waves ($I = 2$) are therefore forbidden. With the realistic interactions, including a tensor component, the first two channels give similar contributions down to about 0.3 MeV. Below that energy, the $^5S_2$ channel overwhelms the $^1D_2$ channel, yielding the flat behavior, whereas above that energy the $^1D_2$ channel contributes more than the $^5S_2$ channel. The $E2$ transition in the case of MN potential occurs through the path (iii), and the corresponding *S*-factor (dotted curve in Fig. 3) is quite similar to the $^1D_2$ contribution of the realistic interactions. The energy-dependence of the *S*-factor, obviously different between the realistic and effective interactions, is

PoS(XXXIV BWNP)008

attributed to the role played by the tensor force. Without the tensor force, we cannot reproduce the ^{2}H$(d,\gamma)^4$He astrophysical S-factor below 0.3 MeV.

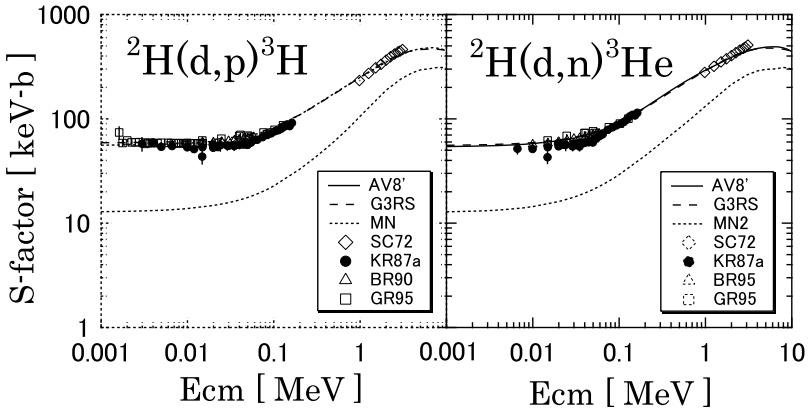

Figure 4: ^{2}H$(d,p)^3$H and ^{2}H$(d,n)^3$He astrophysical S-factors calculated with the realistic (AV8′, G3RS) and the effective (MN) potentials. See Ref. [62] for the experimental data.

Similar conclusions can be drawn for the ^{2}H$(d,p)^3$H and ^{2}H$(d,n)^3$He transfer reactions at low energies. The S factors are presented in Fig. 4. They mainly occur from the transitions of the $d+d$ $^5S_2$ channel to the D-wave continuum of $p+^3$H or $n+^3$He, which is also due to the tensor force. Without the tensor force, these cross sections cannot be reproduced.

5. Conclusion

Nuclear astrophysics is a broad field, where many nuclear inputs are necessary. In particular, charged-particle cross sections are quite important, and difficult to measure, owing to the low energies and cross sections. Cluster models are well adapted to these reactions, since in the low-mass region, the number of open channels is fairly small. The assumption of a cluster structure is in general realistic and allows to find approximate solutions of then A-body Schrödinger equation. Many applications have been performed so far in nuclear astrophysics. One of the future challenges for these models is the use of more realistic nucleon-nucleon interactions, and their extension to higher mass systems.

In this work, we were only concerned with reactions, without discussing other aspects, such as masses, beta decays, etc. In general, charged-particle induced reactions occur at energies much lower than the Coulomb barrier, and the corresponding cross sections are therefore extremely small. An other characteristic is that there is almost no systematics. In the low-mass region, each reaction presents its own peculiarities and difficulties, in the theoretical as well as in the experimental viewpoints. Nevertheless some hierarchy can be established among reactions of astrophysical interest. Transfer reactions, arising from the nuclear interaction, present cross sections larger than capture cross sections which have an electromagnetic origin. In addition, the resonant or non-resonant nature of a reaction also affects the cross section.

We have discussed different theoretical models often used in nuclear astrophysics. The potential model and the R-matrix method are widely applied in this field; they are fairly simple and well

PoS(XXXIV BWNP)008

adapted to low-energy reactions. On the other hand microscopic cluster models have a stronger predictive power, since the only rely on a nucleon-nucleon interaction, and on the assumption of a cluster structure for the nucleus.

A very impressive amount of work has been devoted to nuclear astrophysics in the last decades. Although most reactions involving light nuclei are sufficiently known, some reactions, such as $^{12}C(\alpha,\gamma)^{16}O$ still require much effort to reach the accuracy needed for stellar models. In the nucleosynthesis of heavy elements (*s* process, *p* process), further problems arise from the level densities and the cross sections should be determined from statistical models. A better knowledge of these cross sections represents a challenge for the future.

Acknowledgments

This text presents research results of the IAP programme P6/23 initiated by the Belgian-state Federal Services for Scientific, Technical and Cultural Affairs.

References

[1] W. A. Fowler, G. R. Caughlan, B. A. Zimmerman, Ann. Rev. Astron. Astrophys. 13 (1975) 69.

[2] D. D. Clayton, *Principles of stellar evolution and nucleosynthesis*, The University of Chicago Press, 1983.

[3] C. Rolfs, W. S. Rodney, *Cauldrons in the Cosmos* (University of Chicago Press).

[4] C. Iliadis, *Nuclear Physics of Stars*, Wiley-VCH Verlag GmbH, 2007.

[5] M. Wiescher, T. Rauscher, Nuclear reactions, in: R. Diehl, D. H. Hartmann, N. Prantzos (Eds.), Astronomy with Radioactivities, Vol. 812 of Lecture Notes in Physics, Springer Berlin / Heidelberg, 2011, pp. 461.

[6] K. Langanke, M. Wiescher, Rep. Prog. Phys. 64 (2001) 1657.

[7] K. Langanke, C. A. Barnes, Nucleosynthesis in the big bang and in stars, in: J. W. Negele, E. Vogt (Eds.), Advances in Nuclear Physics, Vol. 22 of Advances in Nuclear Physics, Springer US, 2002, pp. 173.

[8] P. Descouvemont, *Theoretical models for nuclear astrophysics*, Nova Science, New York, 2003.

[9] P. Descouvemont, T. Rauscher, Nucl. Phys. A 777 (2006) 137.

[10] A. M. Lane, R. G. Thomas, Rev. Mod. Phys. 30 (1958) 257.

[11] P. Descouvemont, D. Baye, Rep. Prog. Phys. 73 (2010) 036301.

[12] D. Baye, P. Descouvemont, Ann. Phys. 165 (1985) 115.

[13] I. Thompson, F. Nunes, *Nuclear Reactions for Astrophysics: Principles, Calculation and Applications of Low-Energy Reactions*, Cambridge University Press, 2009.

[14] K. Wildermuth, Y. C. Tang, *A Unified Theory of the Nucleus*, Vieweg, Braunschweig, 1977.

[15] K. Langanke, Adv. In Nucl. Phys., Vol. 21 (1994) 85.

[16] W. Hauser, H. Feshbach, Phys. Rev. 87 (1952) 366.

[17] T. Rauscher, F.-K. Thielemann, At. Data Nucl. Data Tables 75 (2000) 1.

PoS(XXXIV BWNP)008

[18] W. Richter, B. A. Brown, A. Signoracci, M. Wiescher, Prog. Part. Nucl. Phys. 66 (2011) 283.

[19] E. G. Adelberger *et al.*, Rev. Mod. Phys 83 (2011) 195.

[20] A. Kievsky, S. Rosati, M. Viviani, L. E. Marcucci, L. Girlanda, J. Phys. G 35 (2008) 063101.

[21] P. Navrátil, R. Roth, S. Quaglioni, Phys. Rev. C 82 (2010) 034609.

[22] E. Caurier, P. Navratil, Phys. Rev. C 73 (2006) 021302.

[23] T. Neff, Phys. Rev. Lett. 106 (2011) 042502.

[24] P. Navrátil, S. Quaglioni, Phys. Rev. C 83 (2011) 044609.

[25] K. Arai, S. Aoyama, Y. Suzuki, P. Descouvemont, D. Baye, Phys. Rev. Lett. (2011) in press.

[26] P. Descouvemont, M. Dufour, Clusters in Nuclei, Vol.2, Springer, 2011.

[27] J. A. Wheeler, Phys. Rev. 52 (1937) 1083.

[28] H. Horiuchi, Prog. Theor. Phys. Suppl. 62 (1977) 90.

[29] A. B. Volkov, Nucl. Phys. 74 (1965) 33.

[30] D. R. Thompson, M. LeMere, Y. C. Tang, Nucl. Phys. A 286 (1977) 53.

[31] Q. K. K. Liu, H. Kanada, Y. C. Tang, Phys. Rev. C 23 (1981) 645.

[32] H. M. Hofmann, G. M. Hale, Nucl. Phys. A 613 (1997) 69.

[33] P. Descouvemont, D. Baye, Nucl. Phys. A 573 (1994) 28.

[34] P. Descouvemont, Nucl. Phys. A 596 (1996) 285.

[35] D. Baye, M. Kruglanski, Phys. Rev. C 45 (1992) 1321.

[36] D. Baye, P. H. Heenen, M. Libert-Heinemann, Nucl. Phys. A 291 (1977) 230.

[37] V. I. Kukulin, V. G. Neudatchin, I. T. Obukhovski, Y. F. Smirnov, *Clusters as Subsystems in Light Nuclei*, ed. by K. Wildermuth and P. Kramer, Vieweg, Braunschweig (1983).

[38] T. A. Tombrello, Nucl. Phys. 71 (1965) 459.

[39] C. Rolfs, Nucl. Phys. A 217 (1973) 29.

[40] B. Buck, R. A. Baldock, J. A. Rubio, J. Phys. G 11 (1985) L11.

[41] A. M. Mukhamedzhanov, C. A. Gagliardi, R. E. Tribble, Phys. Rev. C 63 (2001) 024612.

[42] A. Azhari, V. Burjan, F. Carstoiu, C. A. Gagliardi, V. Kroha, A. M. Mukhamedzhanov, F. M. Nunes, X. Tang, L. Trache, R. E. Tribble, Phys. Rev. C 63 (2001) 055803.

[43] C. Angulo, P. Descouvemont, Phys. Rev. C 61 (2000) 064611.

[44] C. R. Brune, Phys. Rev. C 66 (2002) 044611.

[45] M. Dufour, P. Descouvemont, Phys. Rev. C 78 (2008) 015808.

[46] C. Angulo, P. Descouvemont, Nucl. Phys. A 639 (1998) 733.

[47] M. F. El Eid, B. S. Meyer, L. S. The, Ap. J. 611 (2004) 452.

[48] P. Dyer, C. A. Barnes, Nucl. Phys. A 233 (1974) 495.

[49] L. Buchmann, Nucl. Phys. A 758 (2005) 355c.

PoS(XXXIV BWNP)008

[50] J. N. Bahcall, S. Basu, M. H. Pinsonneault, Phys. Lett. 433B (1998) 1.

[51] A. R. Junghans, E. C. Mohrmann, K. A. Snover, T. D. Steiger, E. G. Adelberger, J. M. Casandjian, H. E. Swanson, L. Buchmann, S. H. Park, A. Zyuzin, A. M. Laird, Phys. Rev. C 68 (2003) 065803.

[52] P. Descouvemont, Phys. Rev. C 70 (2004) 065802.

[53] J. A. Brown, F. D. Becchetti, J. W. Jänecke, K. Ashktorab, D. A. Roberts, J. J. Kolata, R. J. Smith, K. Lamkin, R. E. Warner, Phys. Rev. Lett. 66 (1991) 2452.

[54] R. J. Smith, J. J. Kolata, K. Lamkin, A. Morsad, F. D. B. andJ. A. Brown, W. Z. Liu, J. W. Jänecke, D. A. Roberts, R. E. Warner, Phys. Rev. C 43 (1991) 2346.

[55] P. Descouvemont, D. Baye, Phys. Lett. B 292 (1992) 235.

[56] H. J. Assenbaum, K. Langanke, C. Rolfs, Z. Phys. A 327 (1987) 461.

[57] K. Sabourov, M. W. Ahmed, S. R. Canon, B. Crowley, K. Joshi, J. H. Kelley, S. O. Nelson, B. A. Perdue, E. C. Schreiber, A. Sabourov, A. Tonchev, H. R. Weller, E. A. Wulf, R. M. Prior, M. C. Spraker, H. M. Hofmann, M. Trini, Phys. Rev. C 70 (2004) 064601.

[58] K. Arai, S. Aoyama, Y. Suzuki, Phys. Rev. C 81 (2010) 037301.

[59] S. Aoyama, K. Arai, Y. Suzuki, P. Descouvemont, D. Baye, Few-Body Syst. (2011) in press.

[60] V. I. Kukulin, V. M. Krasnopol'sky, J. Phys. A 10 (1977) 33.

[61] K. Varga, Y. Suzuki, R. G. Lovas, Nucl. Phys. A 571 (1994) 447.

[62] C. Angulo *et al.*, Nucl. Phys. A 656 (1999) 3.

[63] B. S. Pudliner, V. R. Pandharipande, J. Carlson, S. C. Pieper, R. B. Wiringa, Phys. Rev. C 56 (1997) 1720.

[64] R. Tamagaki, Prog. Theor. Phys. 39 (1968) 91.

[65] M. O. Y. Suzuki, W. Horiuchi, K. Arai, Few-Body Syst. 42 (2008) 33.

[66] E. Hiyama, B. F. Gibson, M. Kamimura, Phys. Rev. C 70 (2004) 031001.

PoS(XXXIV BWNP)008